Acta Crystallographica Section B
Structural Science
ISSN 0108-7681

Revision of the structure of $Cs_2CuSi_5O_{12}$ leucite as orthorhombic *Pbca*

A. M. T. Bell,[a]*‡ K. S. Knight,[b] C. M. B. Henderson[a,c] and A. N. Fitch[d]

[a]Department of Photon Sciences, STFC Daresbury Laboratory, Warrington WA4 4AD, England, [b]ISIS, STFC Rutherford Appleton Laboratory, Didcot OX11 0QX, England, [c]School of Earth, Atmospheric and Environmental Sciences, University of Manchester, Manchester M13 9PL, England, and [d]ESRF, 6 Rue Jules Horowitz, BP 220, 38043 Grenoble Cedex 9, France

‡ Current address: HASYLAB, Deutsches Elektronen-Synchrotron, Notkestrasse 85, 22607 Hamburg, Germany.

Correspondence e-mail: ynotlleb1@mac.com

Received 11 September 2009
Accepted 21 December 2009

The crystal structure of a hydrothermally synthesized leucite analogue $Cs_2CuSi_5O_{12}$ has been determined and refined using the Rietveld method from high-resolution synchrotron X-ray and neutron powder diffraction data. This structure is based on the topology and cation-ordering scheme of the *Pbca* leucite structure of $Cs_2CdSi_5O_{12}$, and exhibits five ordered Si sites and one ordered Cu tetrahedrally coordinated (*T*) site. This structure for $Cs_2CuSi_5O_{12}$ is topologically identical to other known leucite structures and is different from that originally proposed by Heinrich & Baerlocher [(1991), *Acta Cryst.* C**47**, 237–241] in the tetragonal space group $P4_12_12$. The crystal structure of a dry-synthesized leucite analogue $Cs_2CuSi_5O_{12}$ has also been refined; this has the $Ia\bar{3}d$ cubic pollucite structure with disordered *T* sites.

1. Introduction

The crystal structure of end-member leucite ($KAlSi_2O_6$) consists of a three-dimensional framework of silicate tetrahedra in which one third of the Si atoms are replaced by Al, with the larger (W) channels through the framework being occupied by the cavity-filling cation K^+, while the smaller (S) channels are vacant. The framework is propagated in three dimensions by linking four and six rings of TO_4 tetrahedra. This crystal structure has the tetragonal $I4_1/a$ space group at ambient temperature and pressure (Mazzi *et al.*, 1976), but is found to undergo a displacive phase transition to the cubic space group $Ia\bar{3}d$ at $\sim$923 K (Wyart, 1940; Taylor & Henderson, 1968). The structure of pollucite, the naturally occurring Cs-rich analogue of leucite ($Cs_{12}Na_4Al_{16}Si_{32}O_{96}\cdot 4H_2O$), has been determined by Beger (1969) in $Ia\bar{3}d$, but another natural pollucite sample has recently been refined in the monoclinic space group *C*2/*c* (Kamiya *et al.*, 2008). In both of these structures Cs and H_2O occupy the *W* sites, and Na the *S* sites. The synthetic end-member pollucite ($CsAlSi_2O_6$) has the $Ia\bar{3}d$ leucite aristotype structure under ambient conditions with Cs occupying the W sites and with the S sites vacant. Tetragonal and cubic leucite structures may also occur if some *T*-site atoms are replaced by trivalent transition elements or divalent cations. These analogues have the stoichiometries $ACSi_2O_6$ and $A_2BSi_5O_{12}$, where *A* is an alkali metal cation (K, Rb, Cs), *B* is a divalent metal cation (Be, Mg, Fe^{2+}, Co, Ni, Zn, Cd), and *C* is a trivalent metal cation (Al, Fe^{3+}; Torres-Martinez & West, 1986, 1989; Bell & Henderson, 1994*a*,*b*; Bell, Henderson *et al.*, 1994; Henderson *et al.*, 1998). All of these structures have disordered framework cations on the tetrahedrally coordinated (*T*) sites.

However, a synchrotron X-ray powder diffraction, electron diffraction and ^{29}Si MAS NMR study of a leucite analogue with the stoichiometry $K_2MgSi_5O_{12}$ (Bell, Henderson *et al.*,

1994) showed that, while a dry-synthesized sample has the $Ia\bar{3}d$ aristotype structure with disordered T cations (Mg and Si), a hydrothermally synthesized sample had a previously unrecorded $P2_1/c$ monoclinic leucite structure. This monoclinic sample has a unit cell with 24 independent oxygen sites, 12 independent T sites [two with Si surrounded by four SiO_4 tetrahedra (denoted Q4Si(4Si) sites), eight with Si surrounded by three SiO_4 and one MgO_4 (Q4Si(3Si,1Mg)), and two with Mg surrounded by four SiO_4 tetrahedra (Q4Mg(4Si)]. In addition, four symmetry-independent extra-framework, cavity cation sites are occupied by K. A similar synchrotron X-ray powder diffraction and ^{29}Si MAS NMR study of the $Cs_2CdSi_5O_{12}$ leucite phase (Bell, Redfern *et al.*, 1994) determined another previously unrecorded structure type belonging to the orthorhombic *Pbca* space group. The unit cell for this structure has 12 independent oxygen sites, six independent T sites [one Q4Si(4Si), four Q4(3Si,1Mg) and one Q4Mg(4Si)] and two independent Cs sites. Two types of four rings occur, one with four Q4Si(3Si,1Cd) and the other with the arrangement Q4Si(4Si)–Q4Si(3Si,1Cd)–Q4Cd(4Si)–Q4Si(3Si,1Cd). One type of six-ring occurs with the linkages Q4Si(4Si)–Q4Si(3Si,1Cd)–Q4Si(3Si,1Cd)–Q4Cd(4Si)–Q4Si(3Si,1Cd)–Q4Si(3Si,1Cd). Rietveld refinement (Bell & Henderson, 1996, 2009) showed that this ordered *Pbca* structure is also found for dry-synthesized leucite analogues with stoichiometries $Cs_2CoSi_5O_{12}$, $Cs_2NiSi_5O_{12}$ and $Cs_2ZnSi_5O_{12}$, and for hydrothermally synthesized leucite analogues with stoichiometries $Rb_2CdSi_5O_{12}$, $Cs_2MnSi_5O_{12}$, $Cs_2MgSi_5O_{12}$ and $Rb_2MgSi_5O_{12}$. A high-temperature, X-ray powder diffraction study (Redfern & Henderson, 1996) showed that the crystal structure of hydrothermal $K_2MgSi_5O_{12}$ exhibits an unquenchable displacive transition from the $P2_1/c$ monoclinic phase to the *Pbca* orthorhombic phase at 622 K in which five pairs of Si (ten sites) and one pair of Mg (two sites) merge to form five Si sites [one Q4Si(4Si), four Q4Si(3Si,1Mg)] and one Mg [Q4Mg(4Si)) site], while two pairs of K sites merge to form one pair in the *Pbca* polymorph. In both of these polymorphs each Mg atom is separated by two Si atoms from the next nearest Mg.

The crystal structures of the different leucite analogues described above are all topologically identical and the space groups $I4_1/a$, *Pbca* and $P2_1/c$ are all isotropy subgroups of the aristotype phase in the space group $Ia\bar{3}d$. All structural varieties have frameworks built up by linking four and six rings of TO_4 tetrahedra. The topology of the *Pbca* structure is shown in Fig. 1 for $Cs_2CdSi_5O_{12}$ leucite viewed down [010]; note that Q4Si(4Si), Q4Si(3Si,1Cd) and Q4Cd(4Si) tetrahedral sites are distinguished with different colours.

A very different cation-ordering scheme has been determined (Heinrich & Baerlocher, 1991) for a hydrothermally synthesized pollucite analogue with the stoichiometry $Cs_2CuSi_5O_{12}$. This structure was refined in the tetragonal space group $P4_12_12$ with the lattice parameters a = 13.5776 (1) and c = 13.6189 (2) Å. However, in this crystal structure the cation-ordering scheme is topologically different to all the other analogous leucite structures and was reported to have a unit cell with 12 independent O sites, a seven T-site ordered framework with six Si sites [three Q4Si(4Si), two Q4Si(3Si,1Cu) one Q4Si(2Si,2Cu)] and one Cu site [Q4Cu(4Si)]; Cu sites are separated by only one Si. This structure also has three distinct Cs sites. In contrast to the *Pbca* leucites this structure has three different four rings with the arrangements [Q4Si(4Si)–Q4Si(3Si,1Cu)–Q4Si(4Si)–Q4Si(3Si,1Cu)], [Q4Si(4Si)–Q4Si(3Si,1Cu)–Q4Cu(4Si)–Q4Si(3Si,1Cu)] and [Q4Si(4Si)–Q4Si(2Si,2Cu)–Q4Cu(4Si)–

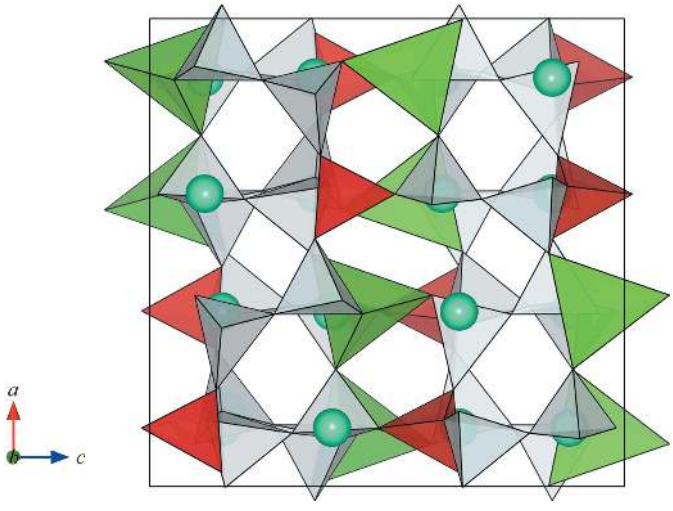

Figure 1
Plot of *Pbca* crystal structure of $Cs_2CdSi_5O_{12}$ (Bell & Henderson, 1994*b*) down [010]. Cs^+ cations are indicated by light blue circles, CdO_4 [Q4Cd(4Si)] by green tetrahedra, Q4Si(4Si) by red tetrahedra and Q4Si(3Si,1Cd) by light grey tetrahedra. Crystal structure plots produced using *VESTA* (Momma & Izumi, 2008).

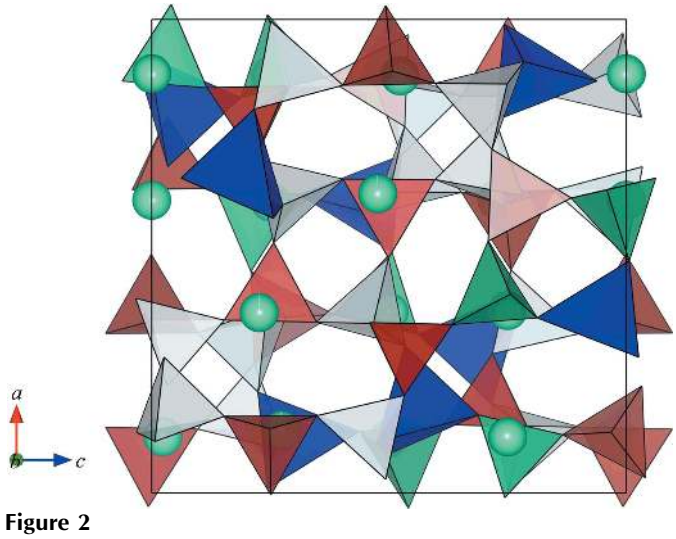

Figure 2
Plot of $P4_12_12$ crystal structure of $Cs_2CuSi_5O_{12}$ (Heinrich & Baerlocher, 1991) down [010]. Cs^+ cations are indicated by light blue circles, CuO_4 [Q4Cu(4Si)] by blue tetrahedra, Q4Si(4Si) by red tetrahedra, Q4Si(3Si,1Cu) by light grey tetrahedra, and Q4Si(2Si,2Cu) by dark green tetrahedra. Note the different arrangement of the Q4Cu(4Si) tetrahedra (blue in this figure) compared with the Q4Cd(4Si) (green) tetrahedra in Fig. 1. The origin is shifted by (1/4, 1/2, 1/8) compared with that for Fig. 1. Crystal structure plots produced using *VESTA* (Momma & Izumi, 2008).

Q4Si(2Si,2Cu)] and has two six rings with the different linkages [Q4Si(4Si)–Q4Si(2Si,2Cu)–Q4Cu(4Si)–Q4Si(3Si,1Cu)–Q4Si(4Si)–Q4Si(3Si,1Cu)] and [Q4Si(4Si)–Q4Si(3Si,1Cu)–Q4Si(4Si)–Q4Si(2Si,2Cu)–Q4Si(4Si)–Q4Si-(3Si,1Cu)]. Fig. 2 shows the structure for $P4_12_12$ $Cs_2CuSi_5O_{12}$ leucite viewed down [010]. The very different framework topologies for Q4Si tetrahedra (Figs. 1 and 2) and for CdO_4 (Fig. 1) and CuO_4 (Fig. 2) tetrahedra are obvious. Note that the origin of the tetragonal crystal structure is displaced from the origin of the aristotype phase in the space group $Ia\bar{3}d$ (and that of the *Pbca* phase) by (1/4, 1/2, 1/8) (Stokes & Hatch, 1988).

In order to assess the likelihood of such fundamentally different structural arrangements for stoichiometrically similar leucite analogues we have synthesized a new sample of hydrothermal $Cs_2CuSi_5O_{12}$ and have determined its crystal structure using both neutron and synchrotron powder diffraction methods. The fact that the sample is dimensionally very close to cubic (c/a = 1.0036) complicates the powder structure determination and necessitates the use of the highest resolution diffraction techniques possible. In addition, another $Cs_2CuSi_5O_{12}$ sample was synthesized under dry conditions at 1 atm. and its structure was determined using synchrotron powder diffraction methods.

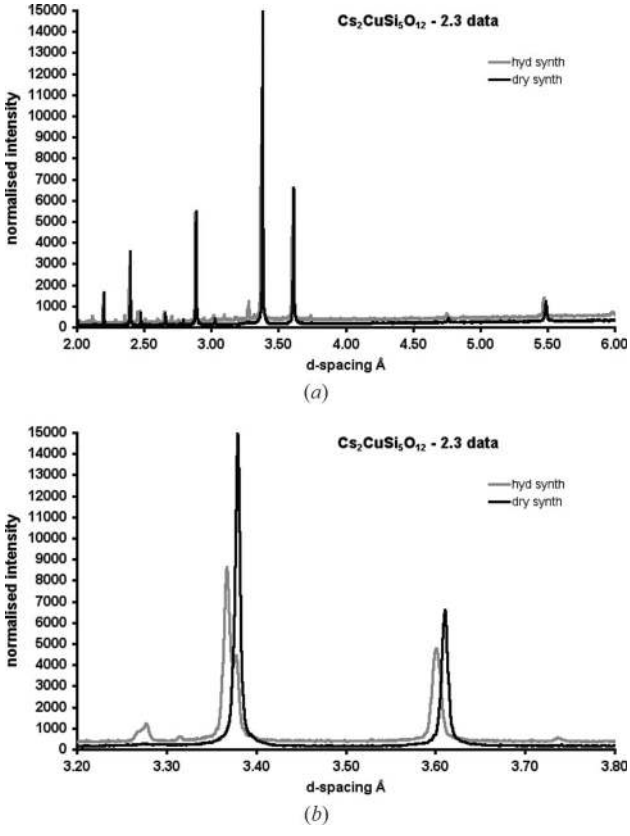

Figure 3
High-resolution powder diffraction data collected on station 2.3 for the dry and hydrothermally synthesized $Cs_2CuSi_5O_{12}$ samples. Fig. 3(*a*) shows data between 2 and 6 Å and Fig. 3(*b*) data between 3.2 and 3.8 Å.

Table 1
Interatomic Cs—O distances for hydrothermal $Cs_2CuSi_5O_{12}$ (Å).

Cs1—O1	3.999 (6)†	Cs2—O1	3.444 (6)
Cs1—O2	3.613 (5)	Cs2—O2	3.958 (6)
Cs1—O3	3.852 (6)	Cs2—O3	3.301 (6)
Cs1—O4	3.434 (5)	Cs2—O4	2.918 (6)
Cs1—O5	3.254 (6)	Cs2—O5	3.413 (5)
Cs1—O6	3.626 (5)	Cs2—O6	3.735 (7)
Cs1—O7	3.152 (6)	Cs2—O7	3.326 (6)
Cs1—O8	3.175 (6)	Cs2—O8	3.786 (6)
Cs1—O9	3.306 (6)	Cs2—O9	3.043 (6)
Cs1—O10	3.589 (6)	Cs2—O10	3.587 (6)
Cs1—O11	3.028 (5)	Cs2—O11	3.616 (7)
Cs1—O12	3.324 (7)	Cs2—O12	3.523 (6)

† Numbers in brackets are 1σ errors in last place(s).

2. Experimental

2.1. Sample preparation

High-purity Cs_2CO_3, CuO and SiO_2 were mixed in stoichiometric proportions and heated in a platinum crucible overnight at 873 K to decompose the carbonate. This mixture was reground, returned to the crucible and melted at 1473 K for 30 min before quenching by dipping the base of the crucible into water. The turquoise-coloured glass was finely ground and used to synthesize the leucite analogues. One sample (denoted CsCu1) was crystallized dry at 1 atmos by heating in a platinum crucible for 3 weeks at 873 K; this product had a turquoise colour similar to that of the glass starting material. The hydrothermal sample (CsCu2) was prepared in four separate $\sim$1 gm batches by sealing in platinum capsules (6 mm diameter, $\sim$ 25 mm long) with $\sim$ 2% added water, and run in cold-seal pressure vessels under the identical conditions of 683 K, 500 bars pressure, for 6 d. Weights of capsules did not change during the experiments showing that they were properly sealed and each sample 'slug' was evenly beige-coloured along its length. X-ray powder diffraction patterns for each of the four batches were identical and the separate samples were then mixed to provide a sufficient sample for neutron diffraction study. Earlier synthesis experiments involved the use of gold capsules (following the method of Heinrich & Baerlocher, 1991), but resulted in very heterogeneous products with dark and light grey, yellow–grey and red regions and these were discarded.

The dry and hydrothermal samples gave similar laboratory X-ray powder diffraction patterns, although the latter had narrower peak shapes indicating better crystallinity. The composition of the hydrothermal sample was determined using electron microprobe methods giving a cell formula (average of 17 spot analyses) of $Cs_{2.02}Cu_{1.00}Si_{4.98}O_{12}$, therefore a stoichiometry of $Cs_2CuSi_5O_{12}$ was assumed.

2.2. Initial synchrotron X-ray powder diffraction

High-resolution synchrotron X-ray powder diffraction data were collected on both the dry synthesized (CsCu1) and hydrothermally synthesized (CsCu2) samples of $Cs_2CuSi_5O_{12}$. Samples were mounted on a flat-plate sample holder and data were collected using the powder diffractometer on station 2.3

of the Daresbury Synchrotron Radiation Source with a synchrotron X-ray wavelength of 1.7974 Å (Cernik *et al.*, 1990; Collins *et al.*, 1992).

Figs. 3(*a*) and (*b*) show plots of these powder data for the two $Cs_2CuSi_5O_{12}$ samples. Note that the dry sample has fewer Bragg peaks than the hydrothermal sample. Fig. 3(*b*) shows Bragg reflections close to 3.38 Å, where the 400/040/004 multiplet would be observed. This is a single peak for the dry sample and a doublet for the hydrothermal sample. This indicates that these two samples do not have the same crystal structures, with the extra Bragg peaks observed for the hydrothermal sample suggesting that this sample has a lower symmetry crystal structure than the dry sample.

Table 2
Interatomic *T*–O (*T*1 = Cu, *T*2–6 = Si) distances for hydrothermal $Cs_2CuSi_5O_{12}$ (Å).

*T*1—O4	1.945 (6)†	*T*4—O2	1.639 (5)
*T*1—O7	1.919 (5)	*T*4—O3	1.595 (5)
*T*1—O9	1.940 (5)	*T*4—O4	1.623 (5)
*T*1—O11	1.853 (5)	*T*4—O12	1.604 (5)
*T*2—O1	1.597 (5)	*T*5—O5	1.634 (5)
*T*2—O3	1.610 (5)	*T*5—O7	1.612 (5)
*T*2—O5	1.630 (5)	*T*5—O8	1.620 (5)
*T*2—O10	1.611 (5)	*T*5—O12	1.645 (5)
*T*3—O1	1.622 (5)	*T*6—O6	1.629 (5)
*T*3—O2	1.613 (5)	*T*6—O8	1.607 (5)
*T*3—O6	1.574 (5)	*T*6—O9	1.645 (5)
*T*3—O11	1.574 (5)	*T*6—O10	1.606 (5)

† Numbers in brackets are 1σ errors in last place(s).

2.3. Neutron and higher-resolution synchrotron X-ray powder diffraction

Owing to the very close overlap of Bragg reflections in the 2.3 synchrotron X-ray powder diffraction data for the hydrothermally synthesized sample it was not possible to carry out a Rietveld structure refinement for this sample with either the *Pbca* leucite structure or the $P4_12_12$ $Cs_2CuSi_5O_{12}$ structure as starting models. Therefore, more powder diffraction data were collected with higher-resolution instruments for the hydrothermal sample $CsCu_2$.

A sample was loaded into an 11 mm outer diameter vanadium can for neutron powder-diffraction data collection using the high-resolution powder diffraction (HRPD) instrument at the ISIS spallation neutron source. Data were collected in time-of-flight mode between 15–215 ms, normalized to the

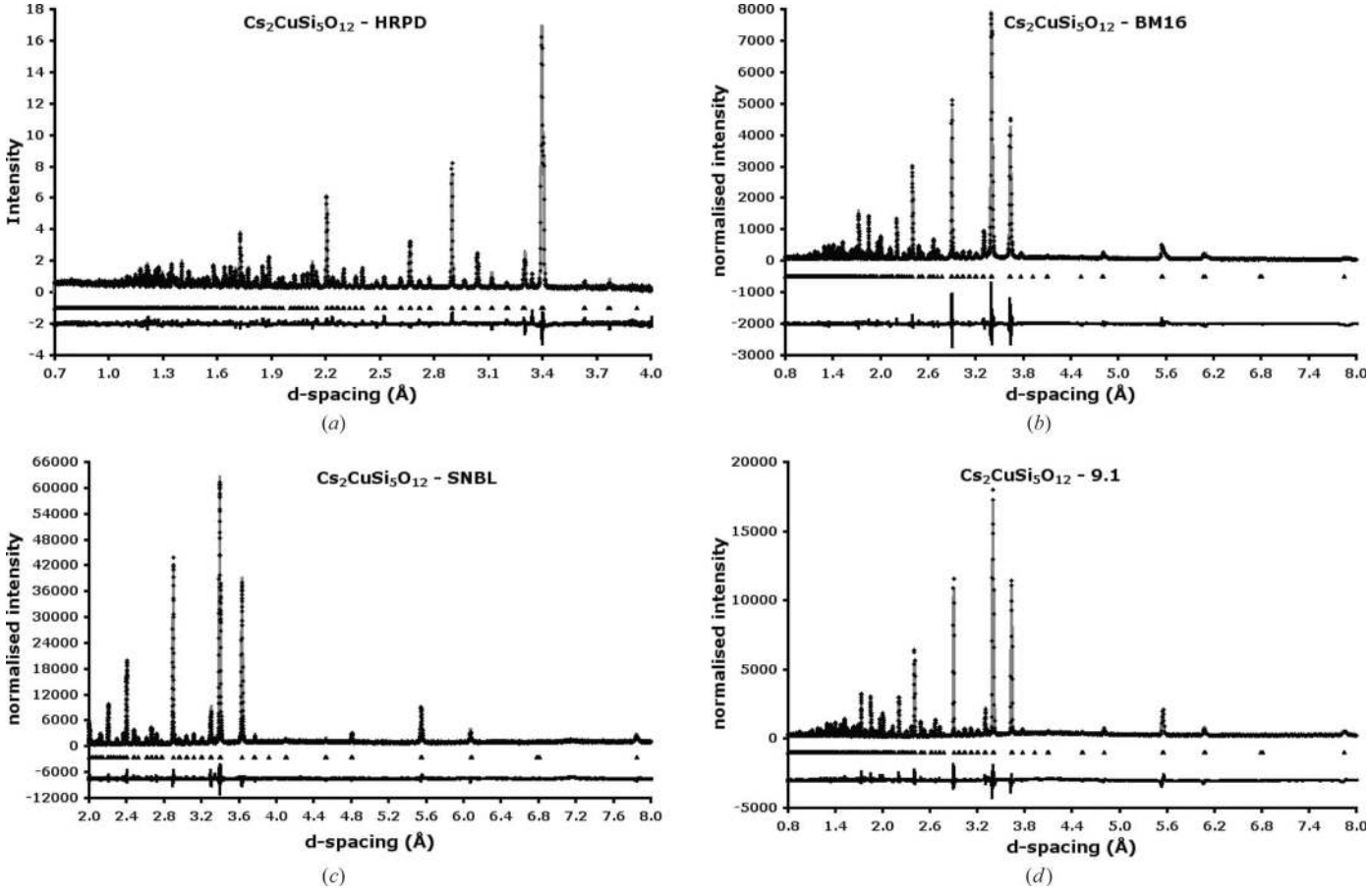

Figure 4
Rietveld difference plots for hydrothermally synthesized $Cs_2CuSi_5O_{12}$, *Pbca* crystal structure. Observed data are indicated by black points, calculated data by a light grey line and the difference plot by a black line. The positions of *Pbca* Bragg reflections are indicated by triangles. Plots are given for data collected on (*a*) HRPD (ISIS), (*b*) BM16 (ESRF), (*c*) SNBL (ESRF) and (*d*) 9.1 (SRS).

Table 3
Interatomic O—*T*—O (*T*1 = Cu, *T*2–6 = Si) angles (°) for hydrothermal $Cs_2CuSi_5O_{12}$.

O4—*T*1—O7	92.3 (2)†	O1—*T*3—O2	114.7 (4)	O5—*T*5—O7	112.9 (4)
O4—*T*1—O9	115.1 (3)	O1—*T*3—O6	94.3 (3)	O5—*T*5—O8	101.1 (3)
O4—*T*1—O11	123.7 (3)	O1—*T*3—O11	108.6 (4)	O5—*T*5—O12	110.0 (4)
O7—*T*1—O9	111.8 (3)	O2—*T*3—O6	111.3 (4)	O7—*T*5—O8	110.9 (4)
O7—*T*1—O11	118.9 (3)	O2—*T*3—O11	110.0 (4)	O7—*T*5—O12	111.1 (4)
O9—*T*1—O11	96.3 (3)	O6—*T*3—O11	117.3 (4)	O8—*T*5—O12	110.4 (4)
O1—*T*2—O3	115.6 (4)	O2—*T*4—O3	103.5 (4)	O6—*T*6—O8	108.7 (4)
O1—*T*2—O5	103.8 (4)	O2—*T*4—O4	113.1 (4)	O6—*T*6—O9	102.4 (4)
O1—*T*2—O10	110.4 (4)	O2—*T*4—O12	106.9 (4)	O6—*T*6—O10	115.3 (4)
O3—*T*2—O5	107.6 (4)	O3—*T*4—O4	117.8 (4)	O8—*T*6—O9	112.4 (4)
O3—*T*2—O10	112.6 (4)	O3—*T*4—O12	100.2 (4)	O8—*T*6—O10	104.6 (4)
O5—*T*2—O10	106.0 (4)	O4—*T*4—O12	114.0 (4)	O9—*T*6—O10	113.6 (4)

† Numbers in brackets are 1σ errors in last place(s).

Table 4
Interatomic *T*—O—*T* (*T*1 = Cu, *T*2–6 = Si) angles (°) for hydrothermal $Cs_2CuSi_5O_{12}$.

*T*2—O1—*T*3	140.8 (4)†	*T*1—O11—*T*3	129.3 (4)
*T*3—O2—*T*4	143.5 (4)	*T*4—O12—*T*5	137.4 (5)
*T*2—O3—*T*4	141.6 (4)	Mean Si—O—Si	144.5
*T*1—O4—*T*4	126.4 (4)	Mean *T*1—O—*T*	130.8
*T*2—O5—*T*5	138.6 (4)	Mean *T*2—O—*T*	144.1
*T*3—O6—*T*6	156.5 (4)	Mean *T*3—O—*T*	142.5
*T*1—O7—*T*5	139.3 (4)	Mean *T*4—O—*T*	137.2
*T*5—O8—*T*6	142.3 (5)	Mean *T*5—O—*T*	140.2
*T*1—O9—*T*6	128.1 (4)	Mean *T*6—O—*T*	145.6
*T*2—O10—*T*6	155.3 (5)		

† Numbers in brackets are 1σ errors in last place(s).

incident flux and corrected for detector efficiency before being rebinned at a resolution suitable for the sample.

Samples were also loaded into 0.5 mm diameter borosilicate glass capillaries for high-resolution synchrotron X-ray powder diffraction data collection. Data were collected on the

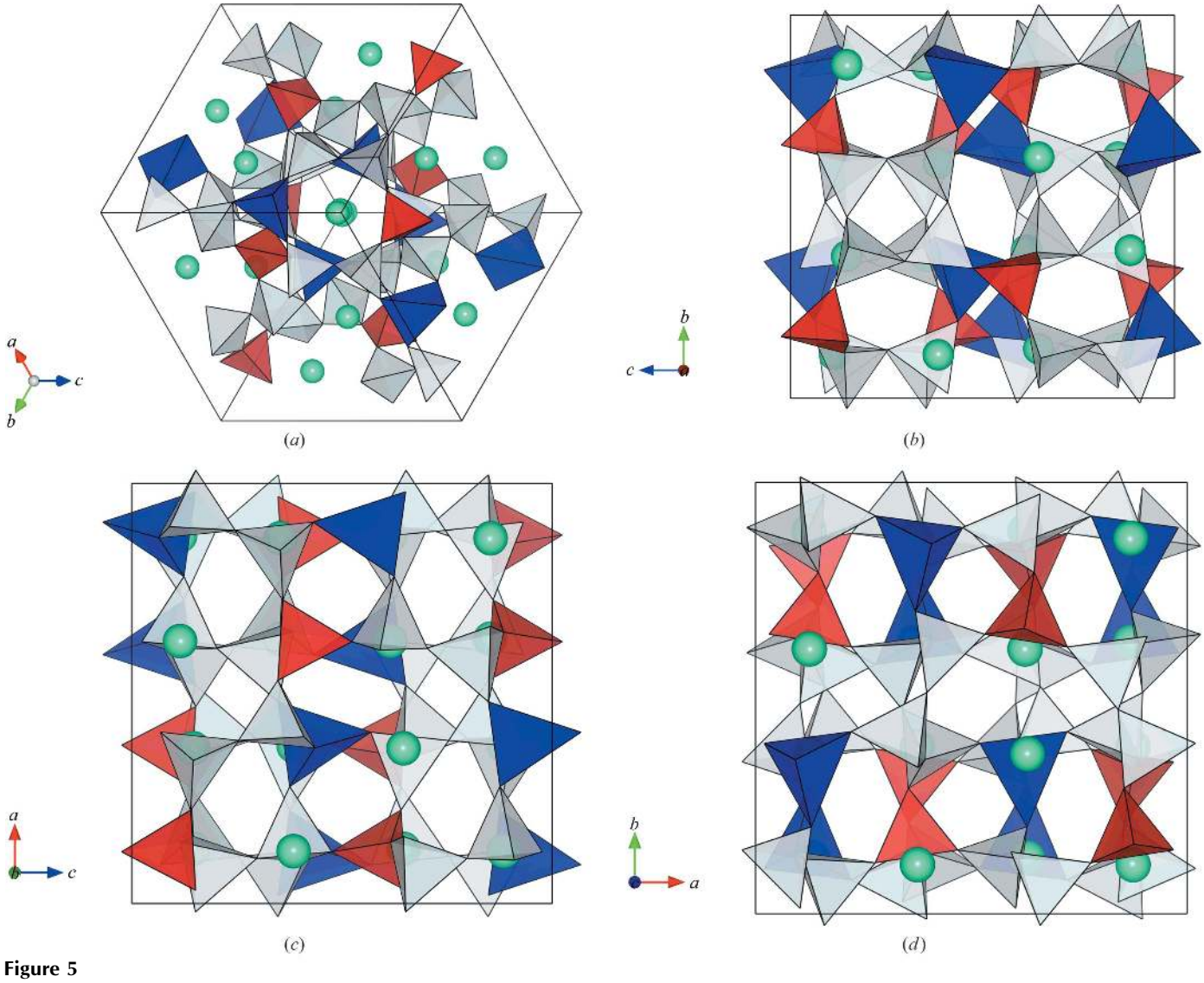

Figure 5
Plot of *Pbca* crystal structure of hydrothermal $Cs_2CuSi_5O_{12}$. Cs^+ cations are indicated by light blue circles, CuO_4 by turquoise tetrahedra, Q4Si(4Si) by red tetrahedra and Q4Si(3Si,1Cu) by light grey tetrahedra: (*a*) down [111]; (*b*) on (100); (*c*) on (010); (*d*) on (001). Crystal structure plots produced using *VESTA* (Momma & Izumi, 2008).

Table 5
Mean Cs—O and *T*—O bond distances (Å), O—*T*—O and *T*—O—*T* angles (°) and tetrahedral site (*T*-site) distortion parameters (deg^2) for *Pbca* $Cs_2CuSi_5O_{12}$ (1σ errors in brackets); *T*1 = Cu, *T*2–6 = Si.

	T—O	O—*T*—O	*T*—O—*T*	*T*-site distortion index (Robinson *et al.*, 1971)	*T*-site NNN connectivity
*T*1—O	1.915 (0.042)	109.6 (12.6)	130.8 (5.8)	159.5	Q4Cu(4Si)
*T*2—O	1.612 (0.014)	109.3 (4.4)	142.1 (11.2)	19.2	Q4Si (4Si)
*T*3—O	1.597 (0.025)	109.4 (8.0)	142.5 (11.2)	64.5	Q4Si(3Si,1Cu)
*T*4—O	1.615 (0.019)	109.3 (6.7)	137.2 (7.7)	46.3	Q4Si (3Si,1Cu)
*T*5—O	1.628 (0.015)	109.4 (4.2)	139.4 (2.1)	17.4	Q4Si (3Si,1Cu)
*T*6—O	1.621 (0.019)	109.5 (5.1)	145.6 (13.3)	26.8	Q4Si (3Si,1Cu)
Mean *T*(2–6)—O	1.615 (0.012)		141.4 (3.2)	34.8 (20.2)	
Mean Si—O—Si			144.5 (7.3)		
Mean Si—O—Cu			130.8 (5.8)		
Mean Cs1—O	3.446 (0.295)				
Mean Cs2—O	3.471 (0.299)				

following powder diffraction instruments: BM16 (λ = 0.354841 Å) and the Swiss–Norwegian beamline (SNBL; λ = 0.80196 Å) at the European Synchrotron Radiation Facility and station 9.1 (λ = 0.993773 Å) of the Daresbury Synchrotron Radiation Source.

2.3.1. Rietveld refinement, hydrothermal sample. Combined neutron and synchrotron X-ray Rietveld (Rietveld, 1969) refinements were carried out using *GSAS* (Larson & Von Dreele, 2004; Toby, 2001). A first refinement was carried out using the *Pbca* structure of $Cs_2CdSi_5O_{12}$ (Bell, Redfern *et al.*, 1994) as a starting model with Cu replacing Cd on the ordered T1 tetrahedral site. Si—O distances were restrained to be 1.62 ± 0.02 Å. No other bond lengths or angles were restrained. Chemically sensible, positive isotropic displacement factors were refined for each site; all five silicon sites were constrained to have the same displacement factor and all 12 oxygen sites were constrained to have the same displacement factor. This refinement converged with R_{wp} = 0.0977, R_p = 0.0712 and χ^2 = 5.018. Bond lengths are given in Tables 1 and 2 and interatomic angles in Tables 3 and 4. Mean bond lengths, angles and distortion parameters for the tetrahedral units are given in Table 5. Fig. 4 shows individual Rietveld difference plots from this refinement and Fig. 5 shows plots of the refined *Pbca* crystal structure for $Cs_2CuSi_5O_{12}$.[1]

In order to assess if the Cu had been placed on the correct *T* site, refinements in the space group *Pbca* were also carried out with Cu ordered onto each of the other *T* sites (*T*2–*T*6) in turn. In each case the isotropic displacement factor for the site containing Cu refined to very large values and those for the sites occupied by Si became negative. As a final test Cu and Si were disordered over the six tetrahedral sites (Si:Cu = 5:1) and the structure was refined with the *T*—O distance restrained to 1.62 Å. In this refinement the T1—O bond distance increased but those for the other *T* sites showed little variation. Thus, the refinement carried out using the $Cs_2CdSi_5O_{12}$ starting model (Cu on *T*1) has the lowest *R* factor and is clearly the most reliable *Pbca* structure for our sample of $Cs_2CuSi_5O_{12}$.

We also refined the crystal structure using the synchrotron and neutron diffraction data sets for our sample of $Cs_2CuSi_5O_{12}$ using the $P4_12_12$ model of Heinrich & Baerlocher (1991), again restraining the Si—O distance to 1.62 Å. This refinement eventually converged with R_{wp} = 0.1318, R_p = 0.0957 and χ^2 = 9.233, but had a negative isotropic displacement factor for the copper site. Based on the quality of fits we believe that the *Pbca* structure model is the correct one for this leucite analogue.

Experimental details for this combined and synchrotron X-ray refinement for the hydrothermal sample are given in Table 6.

2.3.2. Rietveld refinement on dry sample. The 2.3 powder data collected on the dry sample could be indexed as a single $Ia\bar{3}d$ cubic phase similar to the structure of pollucite (Beger, 1969), synthetic leucites $Rb_2ZnSi_5O_{12}$, $CsFeSi_2O_6$ and dry-synthesized $K_2MgSi_5O_{12}$ (Bell & Henderson, 1994*a*,*b*; Bell, Henderson *et al.*, 1994).

A Rietveld refinement (Rietveld, 1969) was carried out using *GSAS* (Larson & Von Dreele, 2004; Toby, 2001). The $Ia\bar{3}d$ cubic structure of $Rb_2ZnSi_5O_{12}$ (Bell & Henderson, 1994*a*) was used as a starting model with Cs replacing Rb as the extra-framework cation and Cu replacing Zn as the disordered framework cation. *T*—O distances (*T* = disordered Cu and Si) were restrained to be 1.6625 ± 0.02 Å. No other bond lengths or angles were restrained. Chemically sensible positive isotropic displacement factors were refined for each site; disordered Si and Cu were constrained to have the same displacement factors. This refinement converged with R_{wp} = 0.1110, R_p = 0.0824 and χ^2 = 2.714. Refined structural parameters for this sample are given in Table 7. Fig. 6(*a*) shows the Rietveld difference plot for this refinement and Fig. 6(*b*) shows a plot of the crystal structure.

Experimental details for this synchrotron X-ray refinement for the dry sample are also given in Table 6.

[1] Supplementary data for this paper are available from the IUCr electronic archives (Reference: HW5006). Services for accessing these data are described at the back of the journal.

Table 6
Experimental details.

Column of parameters for the $Cs_2CuSi_5O_{12}$ hydrothermal synthesized sample is for a combined neutron and synchrotron refinement. Cells in the table are split into four rows corresponding to the four histograms in the *GSAS* Rietveld refinement. Histogram 1 was for neutron powder data collected on HRPD at ISIS. Histogram 2 was for synchrotron X-ray powder diffraction data collected on the Swiss–Norwegian Beam Line at the ESRF. Histogram 3 was for synchrotron X-ray powder diffraction data collected on BM16 at the ESRF. Histogram 4 was for synchrotron X-ray powder diffraction data collected on station 9.1 at the Daresbury SRS. For the cell labelled '*R* factors and goodness of fit' overall *R* factors are given above those for the four individual histograms.

	$Cs_2CuSi_5O_{12}$ hydrothermal synthesized	$Cs_2CuSi_5O_{12}$ dry synthesized
Crystal data		
Chemical formula	$Cs_2CuO_{12}Si_5$	$Cs_8Cu_4O_{48}Si_{20}$
M_r	661.77	2647.08
Crystal system, space group	Orthorhombic, *Pbca*	Cubic, $Ia\bar{3}d$
a, *b*, *c* (Å)	13.58943 (6), 13.57355 (5), 13.62296 (4)	13.6322 (4), 13.6322, 13.6322
V (Å^3)	2512.847 (13)	2533.4 (2)
Z	8	2
Radiation type	Neutron time-of-flight Synchrotron X-ray , λ = 0.80196 Å Synchrotron X-ray , λ = 0.354841 Å Synchrotron X-ray , λ = 0.993773 Å	Synchrotron X-ray , λ = 1.7974 Å
μ (mm^{-1})	0.049915 Unknown −0.59688*E*-02 0.75240*E*-03	N/A flat plate sample
Specimen shape, size (mm)	Cylinder 11 mm diameter, height not known Capillary, 0.5 mm diameter Capillary, 0.5 mm diameter Capillary, 40 mm long, 0.7 mm diameter	Flat sheet, 25 × 0.5
Data collection		
Diffractometer	In-house design In-house design In-house design In-house design	In-house design
Specimen mounting	Vanadium sample can Capillary Capillary Capillary	'Silicon flat-plate sample holder'
Data collection mode	Transmission	Reflection
Data collection method	Time-of-flight Step Step Step	Step
Absorption correction	Debye–Scherrer absorption correction No correction Debye–Scherrer absorption correction Debye–Scherrer absorption correction	No correction
No. of measured, independent and observed reflections	Unknown	–
2θ values (°)	Time of flight $2\theta_{min}$ = 5.000, $2\theta_{max}$ = 40.406, $2\theta_{step}$ = 0.002 $2\theta_{min}$ = 1.002, $2\theta_{max}$ = 45.762, $2\theta_{step}$ = 0.003 $2\theta_{min}$ = 2.01, $2\theta_{max}$ = 80, $2\theta_{step}$ = 0.01	$2\theta_{min}$ = 15.02, $2\theta_{max}$ = 80, $2\theta_{step}$ = 0.01
Refinement		
R factors and goodness-of-fit	R_p = 0.0712, R_{wp} = 0.0977, χ^2 = 5.018 R_p = 0.0833, R_{wp} = 0.0914, R_{exp} = 0.0285, $R(F^2)$ = 0.17158 R_p = 0.069, R_{wp} = 0.0918, R_{exp} = 0.0614, $R(F^2)$ = 0.0386 R_p = 0.083, R_{wp} = 0.1035, R_{exp} = 0.0444, $R(F^2)$ = 0.0928 R_p = 0.0773, R_{wp} = 0.1088, R_{exp} = 0.0520, $R(F^2)$ = 0.11985	R_p = 0.0824, R_{wp} = 0.1110, R_{exp} = 0.067, $R(F^2)$ = 0.05163, χ^2 = 2.714
No. of reflections/data points	3977/6236 257/17704 2956/14921 2850/7800	43/6499

3. Results and discussion

3.1. Hydrothermally synthesized $Cs_2CuSi_5O_{12}$

The structural data obtained for hydrothermally synthesized $Cs_2CuSi_5O_{12}$ based on the four datasets is of a strikingly high quality (owing to the combination of high-resolution synchrotron and neutron data) for a powder diffraction determination with absolute errors of ~ 0.005 Å for individual cation–O bond lengths (relative errors of 0.33% for Si, 0.25% for Cu and 0.2% for Cs). Absolute errors for bond angles are $\sim 0.4^\circ$ (relative errors of 0.4% for O—*T*—O and 0.3% for *T*—O—*T* angles). These errors are ~ 3 to 8 times smaller than previously published powder structural data for leucite bond lengths, and $\sim$ 3–6 times smaller than equivalent bond angles (*e.g.* Bell, Henderson *et al.*, 1994; Bell & Henderson, 1996; Heinrich & Baerlocher, 1991; Bell & Henderson, 2009). We are confident, therefore, that the data for $Cs_2CuSi_5O_{12}$ provide a good basis for characterizing the detailed structural properties of Cs-leucite analogues with ordered *T* cations.

Fig. 5 displays the *Pbca* structure of $Cs_2CuSi_5O_{12}$ projected down [111] (Fig. 5*a*) and down [100], [010] and [001] (Figs. 5*b*, *c* and *d*, respectively). Fig. 5(*a*) shows that the channels in the framework occupied by the large alkali cations are defined by six rings of tetrahedra with Q4Cu(4Si) and Q4Si(4Si) opposite each other and separated by two pairs of connected Q4Si(3Si,1Cu) tetrahedra. The other structure projections show that the framework is built up by linking four and six rings of tetrahedra. The four rings aligned approximately in the (100) plane (shaded grey in Fig. 5*b*) contain only Q4Si(3Si,1Cu) tetrahedra.

Table 6 (continued)

	$Cs_2CuSi_5O_{12}$ hydrothermal synthesized	$Cs_2CuSi_5O_{12}$ dry synthesized
No. of parameters	110	20
No. of restraints	20	8

Computer programs: local software, *GSAS* (Larson & Von Dreele, 2004), *EXPGUI* (Toby, 2001), *VESTA* (Momma & Izumi, 2008), *enCIFer* (CCDC, 2008).

Table 7
Refined interatomic distances and angles for dry-synthesized $Cs_2CuSi_5O_{12}$.

T = disordered Cu (occ = 1/6) and Si (occ = 5/6).

Cs—O ×6	3.363 (5)†	O—T—O	106.4
Cs—O ×6	3.528 (5)	O—T—O	112.0 (3) ×2
T—O ×2	1.631 (4)	O—T—O	101.3 (4)
T—O ×2	1.652 (5)	Mean O—T—O	109.5
O—T—O	112.6 (3) ×2	T—O—T	142.9 (3)

† Numbers in brackets are 1σ errors in last place(s).

In contrast, the four rings approximately parallel to (010) and (001) (Figs. 5*b* and *c*) contain one CuO_4 tetrahedron (blue) opposite a Q4Si(4Si) tetrahedron (red), separated by Q4Si(3Si,1Cu) tetrahedra. The fact that the CuO_4 tetrahedron is significantly larger than SiO_4 tetrahedra leads to the four rings in Figs. 5(*c*) and (*d*) being more distorted than the almost square, Cu-free, four-rings shown in Fig. 5(*b*) (*cf.* $Cs_2CdSi_5O_{12}$; Bell, Redfern *et al.*, 1994).

The mean bond distances and bond angles, and tetrahedral distortion parameters (Robinson *et al.*, 1971) for the *Pbca* structure for $Cs_2CuSi_5O_{12}$ are given in Table 5. The mean Cs—O bond lengths for both alkali sites are identical within error and average 3.46 Å; this defines the lower end of the range of mean Cs—O distances reported for $Cs_2BSi_5O_{12}$ leucites with B = Mg, Zn, Cd, Mn, Ni and Co (3.46–3.54 Å; Bell *et al.*, 1994; Bell & Henderson, 1996, 2009). The well defined value of 3.46 Å is equivalent to an ionic radius for Cs^+ of 2.1 Å, which is 10% larger than Shannon's (1976) value of 1.88 Å for 12-coordinated Cs^+. Note that our value is close to the mean Cs—O distance of 3.48 Å to the 12 closest O atoms for pollucite (Beger, 1969; Palmer *et al.*, 1997).

The mean Cu—O distance of 1.915 Å is equivalent to an ionic radius of 0.565 Å for Cu^{2+} in fourfold coordination matching the value of 0.57 Å given by Shannon (1976). The individual Si—O distances for *T*2–*T*6 sites cover the range 1.57–1.65 Å and fall just outside the range usually found in silicate structures (1.59–1.63 Å; *International Tables for X-ray Crystallography*, 1985, Vol. III, Table 4.1.1). Based on these more precise data for $Cs_2CuSi_5O_{12}$ it seems likely that Si—O values reported for other $Cs_2BSi_5O_{12}$, which are outside this range (*e.g.* 1.51 and 1.67 Å in $Cs_2CdSi_5O_{12}$; Bell, Redfern *et al.*, 1994) are likely to reflect higher experimental errors.

The CuO_4 tetrahedron has a significantly higher O—T—O tetrahedral angle variance (160 deg^2, Table 5; Robinson *et al.*, 1971) than those for BO_4 tetrahedra in other $Cs_2BSi_5O_{12}$ leucites, but this relationship is not simply related to ionic size [*cf.* Cd 94 (Bell, Redfern *et al.*, 1994); Mn 58, Co 60, Ni 47 (Bell & Henderson, 1996); Mg 80 deg^2 (Bell & Henderson, 2009)]. The O—T—O angle variance for the CuO_4 tetrahedron is also substantially higher than the variances for all the SiO_4 tetrahedra in $Cs_2CuSi_5O_{12}$ leucite [range 17.4–64.5 deg^2 (mean 34.8), Table 5], which is opposite the relationships found for other Cs 3*d* transition-element (Mn, Co, Ni) leucites (Bell & Henderson, 1996). Based on the higher quality of the data for $Cs_2CuSi_5O_{12}$ leucite, especially where neutron diffraction data will define the positions of O atoms more reliably than X-ray methods, it seems likely that our earlier determinations suggesting that SiO_4 tetrahedra are more distorted than BO_4 tetrahedra are likely to be in error.

The mean Si—O—Si angle for $Cs_2CuSi_5O_{12}$ has a larger value (144.5°) than that for Si—O—Cd (130.8°) and this is the same relationship found for other $Cs_2BSi_5O_{12}$ leucites: *i.e.* for B = Cd (147 and 127°); Mn (137, 133°); Co (137, 135°); Ni (142, 134°); and for Mg (146, 143°). In all cases B—O distances are larger than those for Si—O and Si—O—B angles are smaller than Si—O—Si angles. In addition, the largest mean B—O

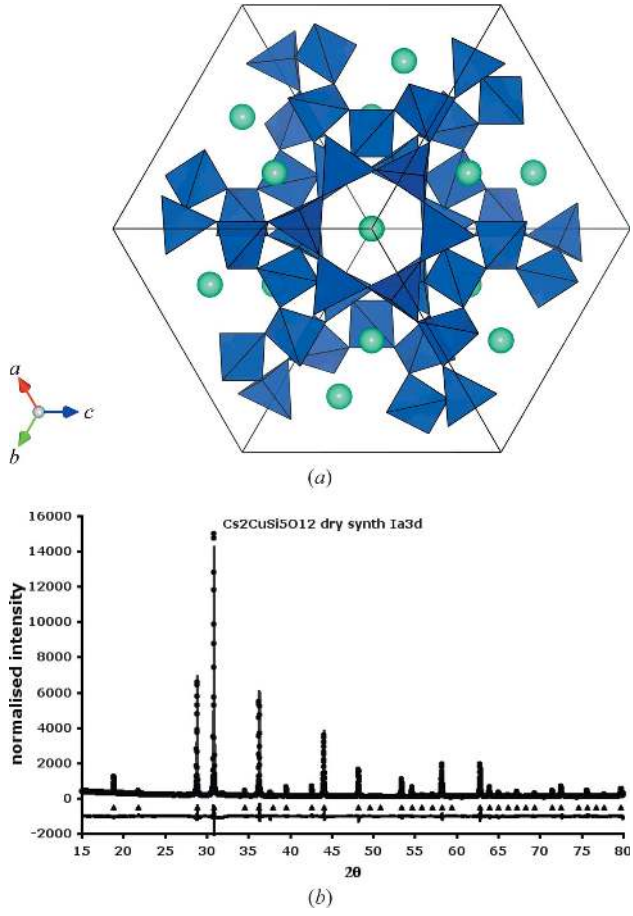

Figure 6
(*a*) Rietveld difference plot for dry-synthesized $Cs_2CuSi_5O_{12}$. Crystal structure plots produced using *VESTA* (Momma & Izumi, 2008). (*b*) Plot of $Ia\bar{3}d$ crystal structure down [111].

distance (Cd—O = 2.24 Å) has the smallest T—O—T (127°) and the smallest B—O (Mg—O = 1.87 Å) has the largest T—O—T (143°). These trends are in agreement with the inverse relationship between mean T—O bond length and mean T—O—T angle shown by framework silicates (Hill & Gibbs, 1979).

3.2. Dry synthesized $Cs_2CuSi_5O_{12}$

The refined crystal structure for the dry-synthesized $Cs_2CuSi_5O_{12}$ sample is similar to that for other $Ia\bar{3}d$ leucites with disordered T-site cations. It should be noted that the unit-cell volume for this disordered polymorph [V = 2533.4 (2) Å^3] is larger than the unit-cell volume for the ordered hydrothermally synthesized polymorph [V = 2512.85 (1) Å^3]. A similar effect was observed in $K_2MgSi_5O_{12}$ [Bell, Henderson *et al.*, 1994; dry sample has V = 2416.33 (5) Å^3, and hydrothermal sample V = 2348 (2) Å^3]. The structures with the ordered cations have more collapsed tetrahedral frameworks and hence smaller unit-cell volumes. As expected, the larger framework collapse for $Cs_2CuSi_5O_{12}$ is reflected in the mean T—O—T angle for the hydrothermal sample (139.9°) being smaller than that for the less-collapsed dry sample (142.9°); this is the same relationship as in $K_2MgSi_5O_{12}$ leucites with values of 137.4 and 144.5° (Bell, Henderson *et al.*, 1994).

4. Conclusions

Rietveld refinement of high resolution, neutron and synchrotron X-ray powder diffraction data for a sample of hydrothermally synthesized $Cs_2CuSi_5O_{12}$ shows that its crystal structure can be better described by the *Pbca* structure rather than by the $P4_12_12$ structure of Heinrich & Baerlocher (1991), which has a much more complicated tetrahedral framework topology. Thus, the tetrahedral cations in $Cs_2CuSi_5O_{12}$ are fully ordered on six T sites, in agreement with the structures of *Pbca* leucites of varying compositions and consistent with the structure of monoclinic $P2_1/c$ leucites with 12 T sites (*e.g.* $K_4Mg_2Si_{10}O_{24}$), which show displacive transitions to *Pbca* polymorphs at elevated temperature. This conclusion follows the famous Ockham's razor dictum 'pluralitas non est ponenda sine necessitate'.

Finally, we note that the space group *Pbca* allows a hypothetical phase transition to the cubic space group $Pa\bar{3}$ at higher temperature. Unlike the phase transition from $P2_1/c$ to *Pbca*, a structural phase transition to $Pa\bar{3}$ from *Pbca* is not permitted to be continuous through either Landau theory or renormalization-group theory (Stokes & Hatch, 1988) and requires the ordered divalent tetrahedral site to become disordered in the cubic space group. We have generated a possible starting model for such a phase using distance least-squares modelling (Baerlocher *et al.*, 1977); this model structure has two independent Cs sites, two independent T sites (disordered Cu and Si) and four independent O sites.

Rietveld refinement of synchrotron X-ray powder diffraction data for a sample of dry synthesized $Cs_2CuSi_5O_{12}$ shows that the structure can be described by the $Ia\bar{3}d$ pollucite structure. In this structure Cu and Si are disordered over the T sites. A high-temperature crystallographic study carried out using high-resolution powder diffraction to assess whether T-site disordering might be associated with a phase transition to either $Pa\bar{3}$ or $Ia\bar{3}d$ would be worthwhile.

We wish to acknowledge the use of the Chemical Database Service at Daresbury (Fletcher *et al.* 1996) and thank John Charnock for carrying out the electron microprobe analysis.

References

Baerlocher, C., Hepp, A. & Meier, W. M. (1977). DLS-76, http://www.crystal.mat.ethz.ch/Software.
Beger, R. M. (1969). *Z. Kristallogr.* **129**, 280–302.
Bell, A. M. T. & Henderson, C. M. B. (1994*a*). *Acta Cryst.* C**50**, 984–986.
Bell, A. M. T. & Henderson, C. M. B. (1994*b*). *Acta Cryst.* C**50**, 1531–1536.
Bell, A. M. T. & Henderson, C. M. B. (1996). *Acta Cryst.* C**52**, 2132–2139.
Bell, A. M. T. & Henderson, C. M. B. (2009). *Acta Cryst.* B**65**, 435–444.
Bell, A. M. T., Henderson, C. M. B., Redfern, S. A. T., Cernik, R. J., Champness, P. E., Fitch, A. N. & Kohn, S. C. (1994). *Acta Cryst.* B**50**, 31–41.
Bell, A. M. T., Redfern, S. A. T., Henderson, C. M. B. & Kohn, S. C. (1994). *Acta Cryst.* B**50**, 560–566.
CCDC (2005). *enCIFer*. Cambridge Crystallographic Data Centre, 12 Union Road, Cambridge, England.
Cernik, R. J., Murray, P. K., Pattison, P. & Fitch, A. N. (1990). *J. Appl. Cryst.* **23**, 292–296.
Collins, S. P., Cernik, R. J., Pattison, P., Bell, A. M. T. & Fitch, A. N. (1992). *Rev. Sci. Instrum.* **63**, 1013–1014.
Fletcher, D. A., McMeeking, R. F. & Parkin, D. J. (1996). *Chem. Inf. Comput. Sci.* **36**, 746–749.
Heinrich, A. R. & Baerlocher, Ch. (1991). *Acta Cryst.* C**47**, 237–241.
Henderson, C. M. B., Bell, A. M. T., Kohn, S. C. & Page, C. S. (1998). *Mineral. Mag.* **62**, 165–178.
Hill, R. J. & Gibbs, G. V. (1979). *Acta Cryst.* B**35**, 25–30.
Kamiya, N., Nishi, K. & Yokomori, Y. (2008). *Z. Kristallogr.* **223**, 584–590.
Larson, A. C. & Von Dreele, R. B. (2004). *GSAS*, Report LAUR 86–748. Los Alamos National Laboratory, New Mexico, USA.
Mazzi, F., Galli, E. & Gottardi, G. (1976). *Am. Mineral.* **61**, 108–115.
Momma, K. & Izumi, F. (2008). *J. Appl. Cryst.* **41**, 653–658.
Palmer, D. C., Dove, M. T., Ibberson, R. M. & Powell, B. M. (1997). *Am. Mineral.* **82**, 16–29.
Redfern, S. A. T. & Henderson, C. M. B. (1996). *Am. Mineral.* **81**, 369–374.
Robinson, K., Gibbs, G. V. & Ribbe, P. H. (1971). *Science*, **172**, 567–570.
Rietveld, H. M. (1969). *J. Appl. Cryst.* **2**, 65–71.
Shannon, R. D. (1976). *Acta Cryst.* A**32**, 751–767.
Stokes, H. T. & Hatch, D. M. (1988). *Isotropy Subgroups of the 230 Crystallographic Space Groups.* Singapore: World Scientific.
Taylor, D. & Henderson, C. M. B. (1968). *Am. Mineral.* **53**, 1476–1489.
Toby, B. H. (2001). *J. Appl. Cryst.* **34**, 210–213.
Torres-Martinez, L. M. & West, A. R. (1986). *Z. Kristallogr.* **175**, 1–7.
Torres-Martinez, L. M. & West, A. R. (1989). *Z. Anorg. Allg. Chem.* **573**, 223–230.
Wyart, M. J. (1940). *Bull. Soc. Miner. Crist.* **63**, 5-17.